

# SHEAR AND COMPRESSION-SHEAR CHARACTERISATION OF A POLYMER MATRIX FOR CARBON FIBRE COMPOSITES

Bohao Zhang<sup>1</sup>, Gustavo Quino<sup>2</sup>, Paul Robinson<sup>3</sup> and Richard Trask<sup>4</sup>

<sup>1</sup> Bristol Composite Institute (BCI), Department of Aerospace Engineering, University of Bristol, Bristol, UK BS1 8TR

<sup>2</sup> The Composite Centre, Department of Aeronautics, Imperial College London, London, UK SW7 2AZ

<sup>3</sup> The Composite Centre, Department of Aeronautics, Imperial College London, London, UK SW7 2AZ

<sup>4</sup> Bristol Composite Institute (BCI), Department of Aerospace Engineering, University of Bristol, Bristol, UK BS1 8TR

**Keywords:** Carbon fibre composites, Polymer matrix, Shear deformation, Compression-shear deformation, Digital image correlation

## ABSTRACT

The compression behaviour of unidirectional carbon fibre/epoxy composites has been widely investigated. The poor compression properties of the material relate to the material instability which leads to the formation of fibre kinkbands. At high fibre volume fractions, this instability results from the polymer matrix which is sheared due to the misalignment of the compressed fibres, culminating in yielding or fracture of the matrix or failure at the matrix-fibre interface. In this study, the shear response of an epoxy polymer matrix under pure shear and shear-compression deformation was investigated. Hollow, thin-walled Prime 27 epoxy specimens were manufactured by machining from cured epoxy cylinders. Experimental results showed that the specimens exhibited a uniform in-plane shear strain in the gauge section in both test modes. The average yield stress of the compression-shear specimens (51.0 MPa) was slightly lower than that of the pure-shear specimens (54.9 MPa), due to the applied compression stress. The shear moduli of the specimens for both test modes were consistent with only 3.8% difference. The applied compression stress delayed the specimen failure and achieved a higher fracture strain. The data collected in these tests will be used in finite element (FE) modelling to explore how the compression behaviour of unidirectional composites can be improved.

## 1 INTRODUCTION

Unidirectional carbon fibre/polymer matrix composites exhibit excellent mechanical properties and thus have been widely used in structural applications. However, these materials show poor mechanical performance upon axial compression due to the material instability which leads to kink band formation [1]. This instability results from the polymer matrix, as the matrix between adjacent misaligned fibres is subjected to a combined compression-shear deformation until the onset of yielding [2]. Works have been conducted to investigate the kinkband formation with the matrix yielding. Experimental and FE results from notched compression test have showed that the formation of a kinkband is associated with matrix yielding by shearing which leads to the development of matrix microcracks, splitting and shear bands [3-4]. Later, an analytical model of the fibre kinkband formation with matrix shearing was proposed [5]. Moreover, a study of the composite strength prediction by considering fibre kinking and matrix shearing when subjected to combined axial compression and in-plane shear deformation has been conducted and showed that the kinkband formation is related with the shear response of the matrix [6]. It is therefore important to characterise the matrix behaviour in pure shear and shear-compression deformation. This data could be used for improved FE modelling of kinkband development in unidirectional carbon fibre/epoxy composites.

The aim of this study was to investigate the shear behaviour of a polymer matrix subjected to pure shear and compression-shear deformation. The shear modulus, shear yield stress and strain, and the post-yielding behaviour of polymer matrix were determined and the influence of compression on this shear

behaviour was investigated. Digital image correlation (DIC) was used to measure the shear strain of the specimens in both test modes.

## 2 EXPERIMENTAL INVESTIGATION

### 2.1 Material

In this study, Prime 27 epoxy resin and slow-curing hardener, supplied by Gurit UK, were used. Both the resin and the hardener were supplied in liquid form. According to the manufacturer's datasheet, the elastic modulus of the cured epoxy is 3.3 GPa and the density is 1.1 g/cm<sup>3</sup>.

### 2.2 Specimen preparation

The shear specimens were manufactured by mixing the epoxy and hardener at the ratio recommended by the epoxy manufacturer, and then degassing in vacuum for 15 minutes until no air bubbles were seen. The resin was then cast into cylinders (25.4 mm in diameter and 53 mm in length) using moulds made by 3D printing. The epoxy was cured at room temperature for 24 hrs, followed by post-curing at 65°C for 7 hrs in a temperature-controlled oven with the use of a thermocouple.

Each post-cured epoxy cylinder was machined to form a hollow, cylindrical configuration with a thin-walled test section as shown in Figure 1. The gauge section had outer diameter of 20.6 mm and an inner diameter of 19.6 mm, resulting in a nominal wall thickness of 0.5 mm.

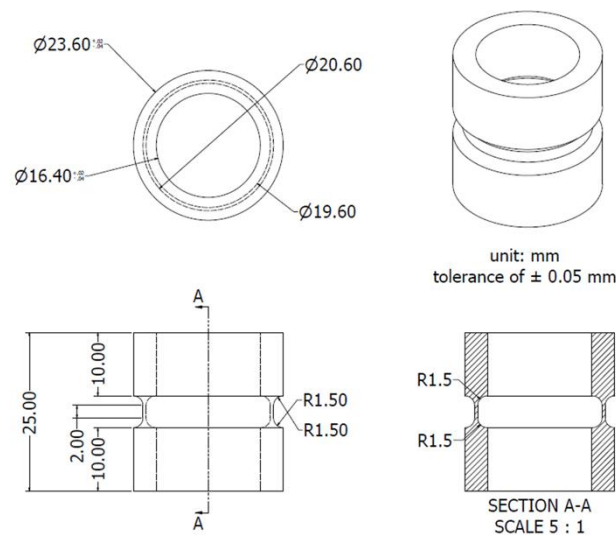


Figure 1: The drawing of the hollow, thin-walled cylindrical specimens for pure shear and compression-shear tests.

The manufactured specimens were CT-scanned to measure the actual wall thickness which was determined to be  $0.51 \pm 0.02$  mm. They were then bonded with endcaps using an epoxy adhesive which was cured at room temperature for 16 h, followed by post-curing in the oven at 80°C for 1 h. Figure 2 shows the drawing of the endcaps and the test fixture used in this work. It can be seen that the endcap contains a hexagonal hole which was fitted to the test fixture. After this, the gauge section of the specimens was sprayed with a thin white layer and then speckled in black using an air brush, for DIC measurement. The specimens were kept in a desiccator prior to testing.

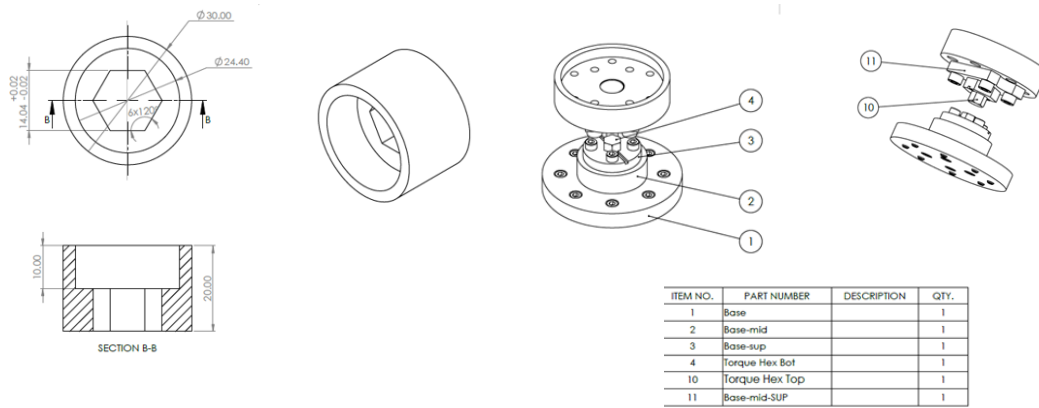


Figure 2: The drawings of endcaps (left) and test fixture (right) used in this work.

### 2.3 Test procedure

Both shear and compression-shear tests were conducted on an Instron Electropuls E10000 fitted with a 10 kN axial and 100 Nm torsional loadcell. As shown in Figure 3, the specimen with the endcaps was mounted onto the bespoke test fixture attached to the crosshead of the test machine. For the pure shear test, the specimen was sheared at a prescribed rotation rate of 0.1 °/s until failure. (A very small compression force of 5 N was applied during these tests.) For the compression-shear tests, a compression force of 660N (corresponding to a stress of 20 MPa) was gradually applied to the specimen over 60 s, while no torsion was applied. (This applied compression stress was well within the elastic behaviour of the epoxy material.) The specimen was then sheared in torsion at 0.1 °/s until failure. Five specimens per test condition were tested. Stereo DIC (LaVision, GE) with two 16-megapixel cameras was used to measure the shear strain within the gauge section of the specimens.



Figure 3: The test setup to conduct pure shear and compression-shear tests.

The shear stress ( $\tau$ ) was determined from the measured torque ( $T$ ) using the thin-walled tube equation (1)

$$\tau = \frac{T}{2\pi\bar{r}^2t} \quad (1)$$

where  $\bar{r}$  = radius at the mid-section of the thin wall and  $t$  = wall thickness of specimens.

The engineering shear strain ( $\gamma$ ) is given by equation (2)

$$\gamma = 2 \times \varepsilon_{xy} \quad (2)$$

where  $\varepsilon_{xy}$  is the shear strain tensor from DIC.

The shear modulus ( $G$ ) of the material is determined from the slope of the shear stress-shear strain plots in the shear strain range 1% - 3%.

### 3 RESULTS

#### 3.1 Pure shear test

Figure 4 shows the shear stress-strain curve of a typical specimen subjected to pure shear deformation. It can be seen that the specimen shows an initially linear shear stress-strain curve, which then yields reaching a maximum stress before a short strain softening stage and then forms a stable plateau, and which is followed by strain hardening stage prior to the formation shear cracks. Following the ASTM D638 standard [7], the onset of yield was determined as the deviation from the linear stress-strain region, and a 0.2% offset was used to determine the associated yield stress and strain values. The resulting yield stress is around 59 MPa at the shear strain of 4.5%. The stress at the yield point (i.e. peak before the plateau) is 75.0 MPa and the corresponding shear strain is 8.2%. The shear modulus from the stresses at 1% to 3% shear strain is 1.43 GPa.

The inserted DIC images show that the in-plane shear strain is constant over the width of the DIC ‘window’ but shows some variation at the upper and lower edges where the window goes beyond the constant thickness gauge section.

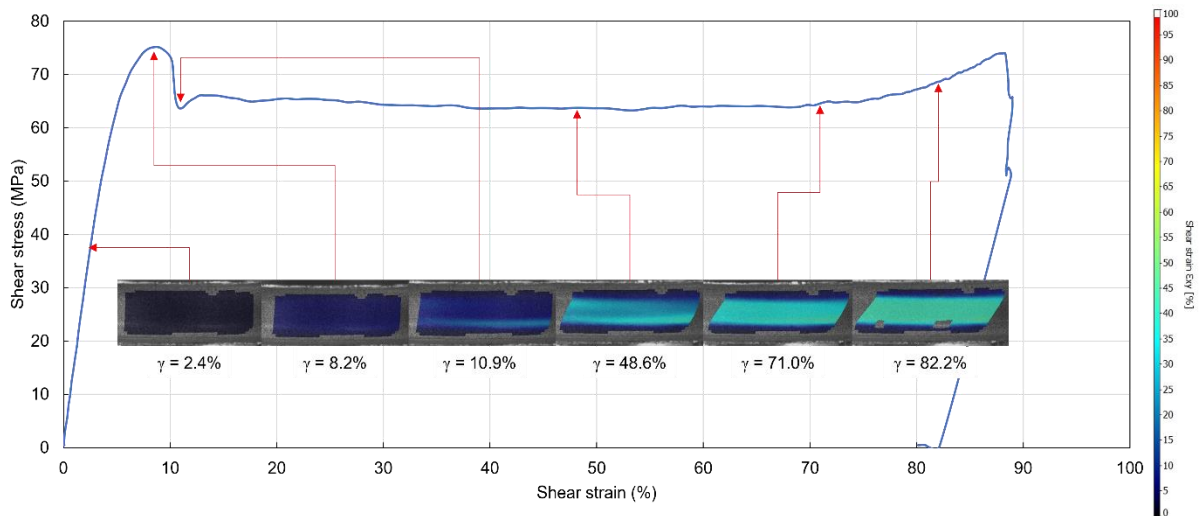


Figure 4: Shear stress-strain relationship of a typical specimen subjected to pure shear deformation with the inserted DIC images to show the in-plane shear strain distribution across the gauge section of the specimen.

### 3.2 Compression-shear test

Figure 5 plots the shear stress as a function of shear strain of a typical specimen tested in the shear-compression mode. The figure shows that the plot has a similar form to that of the pure shear test. The yield strength, again using at 0.2% offset, is 49.6 MPa at a shear strain of 4.5%. The peak stress at the yield point is 68.5 MPa and the associated strain is 10.1%. The shear modulus of the specimen determined between 1% to 3% shear strain is 1.39 GPa.

The inserted DIC images at different shear strains showed that the in-plane shear strain was in general uniform at the section of the constant wall thickness. Again, a strain variation is captured at the upper and lower edges beyond the constant wall thickness region.

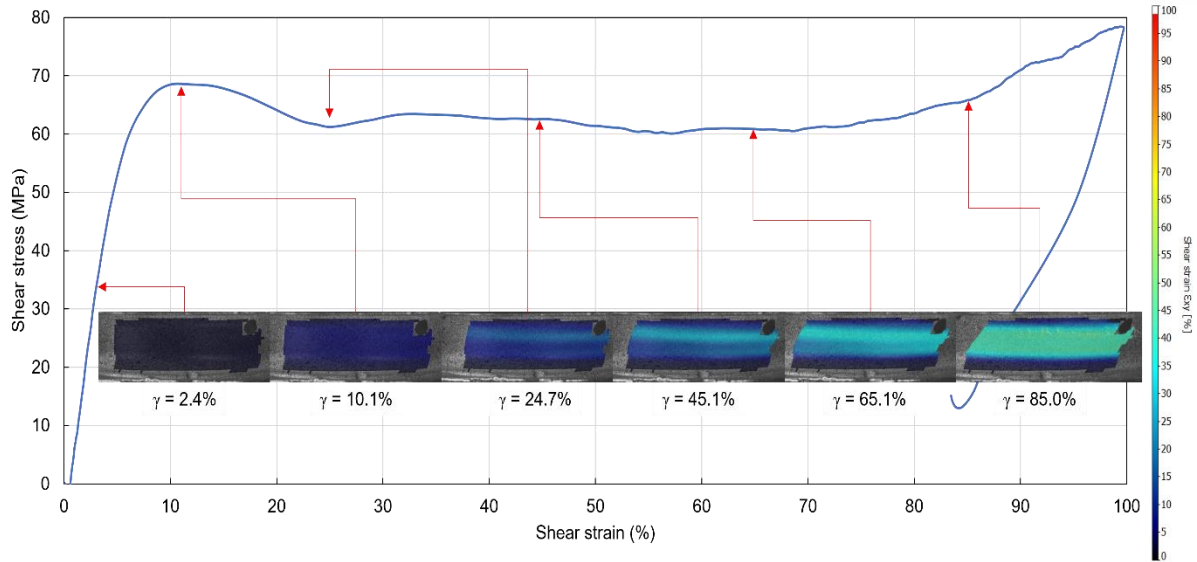


Figure 5: Shear stress-strain relationship of a typical specimen subjected to compression-shear deformation with the inserted DIC images to show the in-plane shear strain distribution across the gauge section of the specimen.

## 4 DISCUSSION

In this work, Prime 27 specimens have been tested in both pure shear and compression-shear deformation to investigate the shear response of the material. Table 1 summarises the average shear modulus, yield stress and strain, and shear stress at fracture of the specimens. It can be seen that the shear moduli from both test modes are consistent (only 3.8% difference between pure shear and compression-shear specimens). However, the pure-shear specimens yielded at slightly higher stress and strain than the compression-shear specimens which indicates the influence of compression loading on the shear behaviour. Upon fracture, the compression-shear specimens exhibit a strain hardening effect which is more significant than for the pure shear test. It seems that the applied compression stress delayed the fracture of the specimen.

Specimens	Average shear modulus (GPa)	Average yield stress (MPa)	Average yield strain (%)	Average shear stress at fracture (MPa)
<i>Machined pure-shear specimens</i>	1.36 ( $\pm$ 0.07)	54.9 ( $\pm$ 3.9)	4.5 ( $\pm$ 0.1)	71.9 ( $\pm$ 2.8)
<i>Machined compression-shear specimens</i>	1.37 ( $\pm$ 0.03)	51.0 ( $\pm$ 2.6)	4.3 ( $\pm$ 0.1)	76.1 ( $\pm$ 2.0)

Table 1: The results of the Prime 27 specimens subjected to pure shear and compression-shear tests. (Results in the bracket are the standard deviation.)

## 5 CONCLUSIONS

In this work, the shear behaviour of an epoxy resin subjected to pure shear and compression-shear deformation has been investigated. In both cases, uniform shear deformation was achieved in the gauge section of the constant wall thickness of the specimens. The applied compression force resulted in a reduction of the yield stress and strain and a more significant strain hardening effect prior to final fracture but had no significant effect on the shear modulus. The data collected in these tests will be used in FE modelling to explore how the compression behaviour of unidirectional composites can be improved.

## ACKNOWLEDGEMENTS

The authors kindly acknowledge the funding for this research provided by UK Engineering and Physical Sciences Research Council (EPSRC) programme Grant EP/T011653/1, Next Generation Fibre-Reinforced Composites: a Full-Scale Redesign for Compression in collaboration with University of Bristol/Imperial College London.

The authors also thank Mr Richard Chaffey for manufacturing shear specimens, and Dr James Thatcher for the Electropuls training.

## REFERENCES

- [1] N.A. Fleck, *Compressive failure of fiber composites*, Advances in applied mechanics, 1997. Publisher Elsevier Science, ISBN 0120020335
- [2] S.T. Pinho, R. Gutkin, S. Pimenta, N.V. De Carvalho and P. Robinson, On longitudinal compressive failure of carbon-fibre-reinforced polymer: from unidirectional to woven, and from virgin to recycled, *Philosophical Transactions of the Royal Society A*, **370**, 2012, pp. 1871–1895 (doi: 10.1098/rsta.2011.0429).
- [3] R. Gutkin, S.T. Pinho, P. Robinson and P.T. Curtis, On the transition from shear-driven fibre compressive failure to fibre kinking in notched CFRP laminates under longitudinal compression, *Composites Science and Technology*, **70**, 2010, pp. 1223-1231 (doi:10.1016/j.compscitech.2010.03.010).
- [4] R. Gutkin, S.T. Pinho, P. Robinson and P.T. Curtis, Micro-mechanical modelling of shear-driven fibre compressive failure and of fibre kinking for failure envelope generation in CFRP laminates, *Composites Science and Technology*, **70**, 2010. pp. 1214-1222 (doi:10.1016/j.compscitech.2010.03.009).
- [5] S. Pimenta, R. Gutkin, S.T. Pinho and P. Robinson, A micromechanical model for kink-band formation: Part II—Analytical modelling, *Composites Science and Technology*, **69**, 2009, pp. 956-964 (doi:10.1016/j.compscitech.2009.02.003).
- [6] R. Gutkin, S.T. Pinho, P. Robinson and P.T. Curtis, A finite fracture mechanics formulation to predict fibre kinking and splitting in CFRP under combined longitudinal compression and in-plane shear. *Mechanics of Materials*, **43**, 2011, pp. 730-739 (doi:10.1016/j.mechmat.2011.08.002).
- [7] ASTM International, ASTM D638-22 Standard Test Method for Tensile Properties of Plastics, West Conshohocken, Pennsylvania, 2023 (DOI: 10.1520/D0638-22).